Structure and energetics of the elbows in the Au(111) herringbone reconstruction

N. C. Bartelt [*] and K. Thürmer [†]

Sandia National Laboratories, Livermore, California 94550, USA

We study the structure of the threading edge dislocations, or "elbows," which are an essential component of the well-known herringbone reconstruction of the (111) surface of Au. Previous work had shown that these dislocations can be stabilized by long-range elastic relaxations into the bulk. However, the validity of the harmonic spring model that had been used to estimate the energies of the dislocations is uncertain. To enable a more refined model of the dislocation energetics, we have imaged the atomic structure of these dislocations using scanning tunneling microscopy. We find that the harmonic spring model does not adequately reproduce the observed structure. We are able to reproduce the structure, however, with a two-dimensional Frenkel-Kontorova (FK) model that uses a pairwise Morse potential to describe the interactions between the top layer Au atoms on a rigid substrate. The parameters of the potential were obtained by fitting the energy of uniaxially compressed phases, or "stripes", computed with density functional theory, as a function of surface Au density. Within this model, the formation of the threading dislocations remains unfavorable. However, the large forces on the substrate atoms near the threading-dislocation cores, render the assumption of a completely rigid substrate questionable. Indeed, if the FK parameters are modified to account for the relaxation of just one more atomic layer, threading dislocations can, in principle, become favorable, even without bulk elastic relaxations. Additional evidence for a small elbow energy is that our computed change in the Au(111) surface stress tensor caused by the $(\sqrt{3} \times 22)$ reconstruction is considerably smaller than previous estimates.

I. INTRODUCTION

The uppermost atomic layers of surfaces and thin films are often reconstructed to have densities different from the bulk crystal. These density modifications can take the form of well-defined misfit dislocations [1]. Such dislocations are important, for example, because of their propensity to change the chemical reactivity of the surface. Indeed, adsorption can even rearrange the dislocations and change their topology and so they are inherent to surface chemical reactivity [2]. Because of their increased ability to enhance surface chemical reactivity, dislocations that locally modify the coordination of atoms are of particular concern. On close-packed surfaces these are "threading" dislocations [1], whose cores run vertically (or "thread") from the surface through the atomic layer(s) with defective in-plane coordination towards the uppermost atomic layer — often the second layer — that preserves the bulk's sixfold in-plane coordination. Although frequently observed [3], current understanding of what determines structure, energetics, and occurrence of these threading dislocations is still rudimentary. The "elbow" dislocations of the much studied [4–11] herringbone reconstruction of Au(111) are a case in point. Figure 1 shows a schematic of the herringbone reconstruction and its various components. Regions I and II are uniaxially compressed in the direction perpendicular to the respective dislocation lines (bright bands in Fig. 1), producing

a $(\sqrt{3} \times 22)$ cell with two atoms added to the 44 atoms of the unreconstructed surface. These regions preserve the sixfold coordination of each surface Au atom with its neighboring surface atoms. Regions III and IV contain elbows, which separate two of the three orientations of the uniaxially compressed $(\sqrt{3} \times 22)$ phase. An essential feature of the elbows are the above-mentioned threading edge dislocations, whose cores run vertically from the surface through the top atomic layer towards the second layer, which in Au(111) is the uppermost atomic layer with bulklike in-plane coordination. These elbow cores can be thought of as endpoints of atom rows inserted into the top layer, producing the Burgers circuits with nonzero Burgers vectors marked blue in Fig. 1. Since the atoms in their core regions are arranged in non-close-packed configurations, such structures are expected to be energetically costly and the reason for their existence is not immediately clear.

The structure of the $(\sqrt{3} \times 22)$ phase in region I and II is well understood. Atoms at the surface lower their energy by being closer to each other than in the bulk, resulting in a higher density of the surface layer compared to the unreconstructed atom layers beneath. The additional surface atoms are most easily accommodated in two-fold coordinated bridge sites separating regions of fcc and hcp stacking, as shown in Fig. 1. The stripes can be thought of as pairs of Shockley partial dislocations [1]. The width of the hcp region depends on the energy cost of the hcp sites compared to the fcc sites. Since interatomic separations in the stripes are still comparatively large in the direction parallel to the stripes, the surface, in principle, could lower its energy by contracting in this

————————
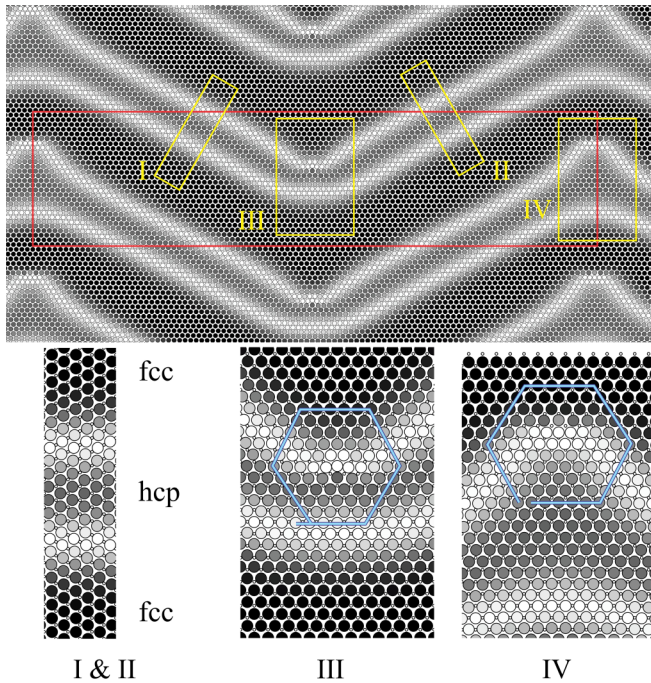*bartelt@sandia.gov
†kthurme@sandia.gov

FIG. 1. Schematic of the herringbone reconstruction. Regions I and II are two rotationally equivalent domains of the ($\sqrt{3} \times 22$) striped, or soliton phase. Regions III and IV are two types of threading edge dislocations.

direction as well. However, to do so would require a fraction of the top layer atoms to occupy very unfavorable sites on the atom layer beneath.

Narasimhan and Vanderbilt [11] used a two-dimensional (2D) Frenkel-Kontorova (FK) model to describe the atomic structure of the elbows in regions Regions III and IV. In their model, a harmonic spring potential is assumed between top layer atoms on a rigid substrate. Because of the large energy cost of the elbows in this 2D model, they proposed that large *bulk* relaxations, which can occur underneath the boundaries between regions of different surface stress, are needed to stabilize the elbows of the herringbone reconstruction. These relaxations can lower the surface energy enough to compensate for the energy cost of creating the defects at the core of the threading edge dislocations. The herringbone reconstruction could thus be understood as an example of spontaneous stress-domain formation, with the lines connecting the cores of the threading edge dislocations representing the domain boundaries. However, the energetic model of the dislocations (as warned in Ref. [11]) is potentially unrealistic, in that it assumes a simple spring interaction between atoms. One thus might question the conclusion that substrate relaxations are necessary to stabilize the threading dislocations, especially because for some systems, models that do not include substrate relaxations have predicted threading dislocations to represent the ground state. For example, Hamilton and Foiles [12], using a strictly 2D model of strained Cu films on Ru(0001), find that a trigon phase, composed of threading dislocations in a triangular arrangement, is favored over the striped phase. Thus threading dislocations can be stable even without substrate relaxations; their stability will depend on the

exact FK parameters, motivating a refined calculation of their values.

Another uncertainty is the validity of the FK model itself. The FK model has provided many valuable insights into the mechanisms of surface reconstructions because of its conceptual simplicity (see, e.g., Ref. [13]). However, its crude implementation of interatomic interactions can potentially miss important physics. Of particular concern here is how the substrate is assumed to apply a (corrugated) potential to the top-layer atoms. The parameters describing this potential are usually obtained by assuming that the atoms below the top layer are fixed in their unreconstructed positions. This assumption is only reasonable if top-layer atoms at the positions predicted by the FK model exert forces on the underlying substrate that would only cause negligible distortions in the atom layer underneath the top layer. For the Shockley partial dislocations in Fig. 1 this is reasonable (as we will show); however, for the elbows the validity of this assumption is uncertain, especially given the hypothesized importance to their stability of long-ranged bulk elastic distortions.

To buttress the development of a robust model we have examined the atomic structure of the cores of the threading dislocations with scanning tunneling microscopy (STM). Two phenomena make these observations difficult. First, these cores are well known sinks of impurity atoms [6]. Second, they can be mobile as Au adatoms can rapidly exchange in and out of them, even at room temperature. As reported below we are able to overcome these challenges and, using scanning tunneling microscopy, report on the detailed structure of one of the two types of threading dislocation, significantly improving on the early observations of Refs. [6,10]. We show, indeed, that the simple spring model cannot reproduce the observed structure, and develop a more refined model that can. The refined model yields elbow energies that are lower than that of the simple spring model, but still increase the energy. However, we argue that if one considers substrate relaxations in the layer below the surface layer, the elbow dislocation energy decreases significantly: such relaxations (which cannot be described by bulk elasticity theory) are needed to account accurately for the stability of the herringbone reconstruction.

II. EXPERIMENT

Exceedingly small amounts of surface impurities, on the order of 0.01 monolayers or less, can have a strong effect on structure and energetics of the herringbone if they are mobile enough to migrate and attach to the threading-dislocation cores [6]. As typically seen in early stages of preparing the Au(111) surface, and systematically studied on another herringbone system, Ag/Ru(0001) [2], trace amounts of impurities that preferentially bind to the dislocation cores, can prevent the formation of or destroy a well-ordered periodic herringbone-reconstructed surface. To overcome these impurity issues, we cleaned the Au sample extensively via multiple cycles of ion bombardment (Ar$^+$, 1 keV) and annealing to ≈800 ºC. Figure 2(a) shows a large-scale image of the resulting well-ordered structure. Figure 2(b) shows an atomic-resolution image of the threading dislocation core denoted IV in Fig. 1. These images were acquired with a low temperature STM (manufactured by CreaTec Fischer & Co. GmbH) at
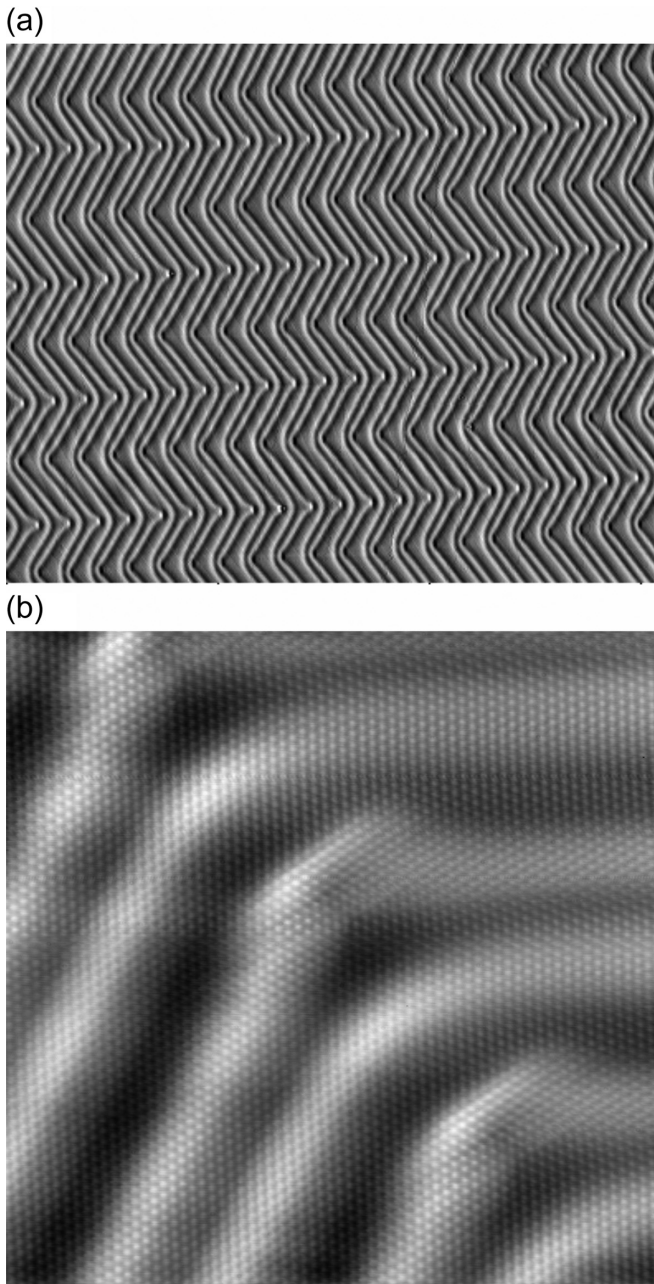
(a)

(b)

FIG. 2. (a) A large-scale STM image (155 nm × 127 nm) of the herringbone reconstruction. Imaging parameters: sample bias $V_t = 0.7$ V; tunneling current $I_t = 500$ pA (b) An atomic-resolution image (16 nm × 16 nm) of the area surrounding region IV of the reconstruction. $V_t = -1.7$ V; $I_t = 300$ pA.
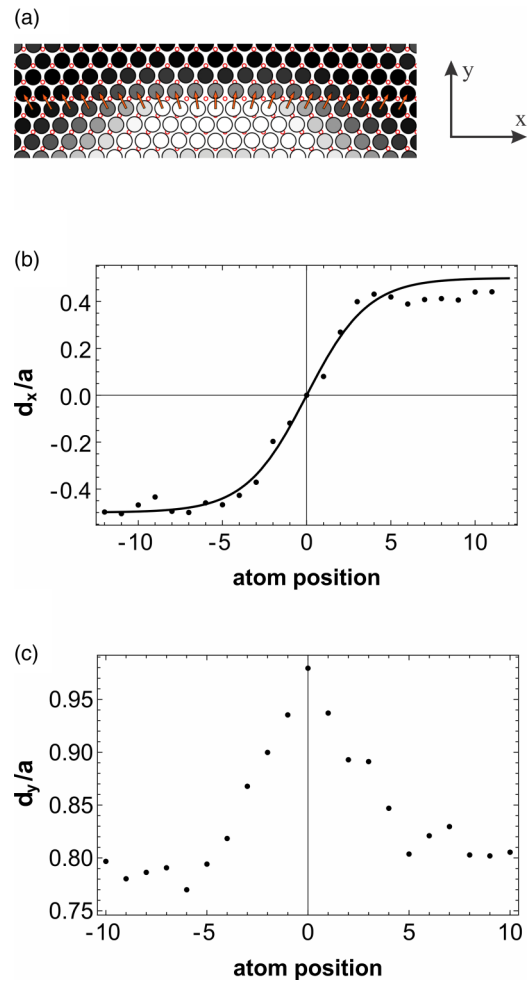
(a)

(b)

(c)

FIG. 3. (a) A schematic showing the atomic displacements we have measured to characterize the dislocation shown in Fig. 2(b). The small red circles represent the positions of the uppermost substrate atoms. (b) Plots the x component of the displacement. The solid line is a fit to a hyperbolic tangent. (c) Plots the y component.

liquid He temperature. At the chosen imaging parameters, sample bias $|V_t| \geqslant 0.5$ V and tunneling current $I_t \leqslant 500$ pA, the gap between STM tip and sample is large enough to avoid tip-induced surface modifications, as evidenced by the lack of image frizziness at the delicate dislocation core. Atomic coordinates were extracted by manually estimating the centers of the small surface protrusions. Distances were calibrated via comparison with the spacing between atom rows along the $\sqrt{3}$ direction parallel to the Shockley partial dislocation lines.

To characterize the elbow structure quantitatively, we determined the vector $\boldsymbol{d}$ separating neighboring Au atoms through the dislocation core. A schematic of this vector is shown in Fig. 3(a). Figures 3(b) and 3(c) plot the two components of the displacement vector $\boldsymbol{d}$ as a function of distance from the core. These results are the average of the measurements from the two cores depicted in Fig. 2(b). Scan direction and shape of the STM tip inevitably introduce some asymmetry into the imaging process, causing a subtle difference in appearance between the bottom left half and top right half of Fig. 2(b). This small imaging artefact, however, does not seem to have a significant effect on the measured displacements d_x and d_y, which both exhibit the expected symmetry around the dislocation core. To quantify the width w of the dislocation core we fit d_x to the form

$$d_x = \left(\frac{a}{2}\right) \tanh\left(\frac{n}{w}\right),$$

where n counts the number of atoms from the dislocation core. The fit gives $w = 3.6 \pm 0.5$.

Our goal is to construct a model that reproduces the measured structure including this value of the dislocation-core width to enable an accurate estimate of the energy of the elbows.

III. FRENKEL-KONTOROVA MODEL OF Au(111)

First we consider the 2D FK model of Au(111) used by Narasimhan and Vanderbilt [11]. The energy in the FK model is the sum of a substrate potential V_s and interaction U between Au atoms in the top layer:

$$E = \sum_i \left[V_s(r_i) + \frac{1}{2} \sum_j U(d_{ij}) \right], \tag{1}$$

where $\mathbf{r}_i$ is the position of the i'th Au atom, and d_{ij} is the distance between atoms i and j.

The substrate potential is taken to be the minimal sum of Fourier components that gives the energy of a (1×1) layer in the hcp sites, bridge sites, and atop sites to be e_h, e_b, and e_t higher per atom than a (1×1) layer in the fcc sites, respectively. This sum is

$$V_s(x, y) = V_0 + \frac{(3e_b + e_t)}{4} - \frac{(e_h - 2e_t)}{9} \left[2\cos(2\pi x)\cos\left(\frac{2\pi y}{\sqrt{3}}\right) + \sin\left(\frac{4\pi y}{\sqrt{3}}\right) \right]$$

$$+ \frac{(4e_h - 9e_b - e_t)}{36}[\cos(4\pi x) + 2\cos(2\pi x)\cos(2\pi\sqrt{3}y)]$$

$$+ \frac{2\sqrt{3}e_h}{9}\sin\left(\frac{4\pi y}{\sqrt{3}}\right)\left[\cos(2\pi x) - \cos\left(\frac{2\pi y}{\sqrt{3}}\right)\right]. \tag{2}$$

Here and below all distances are given in units of the Au bulk nearest neighbor distance $a = 2.884$ Å. The offset V_0 is fixed by the requirement that adding one (1×1) layer in the fcc sites increases the number of bulk layers by one. Defining the zero of energy of Au atoms to be the energy per atom thus requires that $E(1 \times 1) = 0$ (and thus $V_0 = -3U$ (1) if U(r) only connects nearest neighbor atoms).

Following the first-principles calculations of Takeuchi, Chan, and Ho [14], Narasimhan and Vanderbilt took e_h, e_b, and e_t to be 12.3, 42.2, and 187.7 meV, respectively. The interactions between Au atoms in the surface layer are assumed to be simple springs with an interaction of the form $U(d) = k(d-b)^2/2$, connecting each atom to its six nearest neighbors. To reproduce the experimentally observed structure of the striped phase, k was taken to be 10.173 eV; and b was chosen to be 0.961997.

We have used this model to determine the predicted atom positions in the dislocation elbows. We used a $(14\sqrt{3} \times 102)$ herringbone unit cell containing 2992 Au atoms, as depicted in Fig. 1. To create the striped and herringbone phases, we inserted rows of atoms into the (1×1) surface and relaxed the atom positions using the conjugate gradient method. Figure 4 shows the resulting displacement vectors of the computed elbow structure. Fitting a hyperbolic tangent to d_x yields a value of $w = 2.1$ for the width of the dislocation core, significantly smaller than the experimental result of 3.6 ± 0.5 in Fig. 3. Furthermore, the variation of d_y is qualitatively different from the experimental result, as revealed by comparing Fig. 4(b) with Fig. 3(c).

Using this 2D model, Narasimhan and Vanderbilt conclude that the herringbone reconstruction is ~0.97 eV per herringbone unit cell higher in energy than the striped phase because of the presence of the two elbows (we have recomputed this energy with our slightly different sized cell, and find an energy difference of 0.93 eV), and thus argue that 3D stress domain relaxations are necessary for the stability of the herringbone structure.

However, the validity of this estimate of the elbow energy is uncertain, given how poorly the spring model reproduces the dislocation structure within the core of the herringbone elbow threading edge dislocations, where each atom does not obviously have six neighbors. Because of the large variety of local atomic environments in the threading dislocation core, creating a realistic model is a difficult problem. We approach
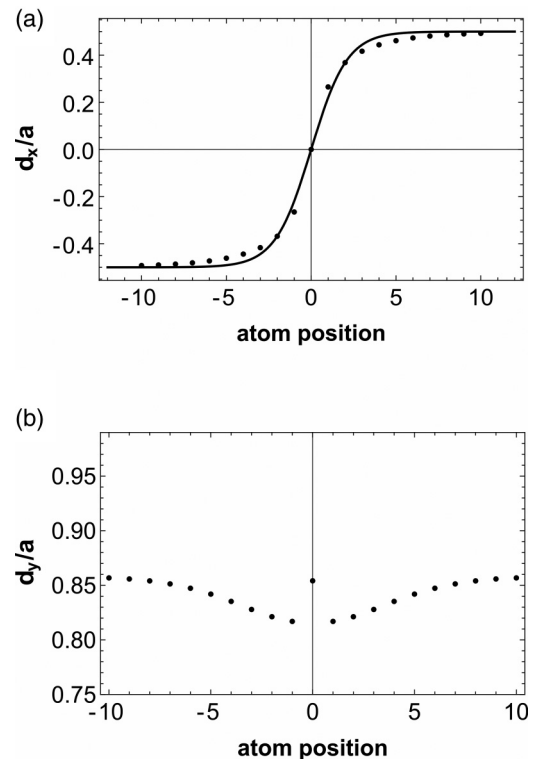

FIG. 4. Variation of the two components of the displacement vector described in Fig. 3(a) for the harmonic FK model. The x component is shown in (a), the y component in (b).

this challenge by designing an interatomic potential for the FK model that behaves more realistically in highly distorted regions, guided by comparison with *ab initio* calculations of several different surface configurations involving stretched and compressed bonds. Assuming springs between widely spaced atoms is clearly problematic because interatomic interactions should eventually decrease with increasing separation. Also, harmonic springs severely underestimate the energy cost of moving atoms very close together, yielding unrealistically dense regions at the dislocation cores. To construct a more reasonable model, following Refs. [15,16], we have used a Morse potential defined by

$$U(r) = -V_0 + V_0(1 - \exp{(-\alpha(r - a_0)/a_0)})^2. \quad (3)$$

To fit the parameters, we adopted the following strategy. We computed the surface energy of uniaxially compressed (striped) phases as a function of their density using density functional theory (DFT) as implemented in the VASP code [17–19]. We used the exchange-correlation functional of Perdew-Burke-Ernzerhof (PBE) [20]. Our calculations were performed for slabs of seven (111) layers and at least 12 Å of vacuum. Atoms in the bottom three layers were held fixed at their bulk equilibrium positions. Dipole corrections were applied to account for this asymmetry of the slab. Surface cell sizes ranging from $(\sqrt{3} \times 10)$ to $(\sqrt{3} \times 30)$ were considered. We used a $(9 \times 2 \times 1)$ k-point and a 700 eV plane-wave cutoff. Forces were relaxed to be less than 0.001 eV/Å. Convergence with respect to all of these parameters was carefully checked. In particular, the results are not sensitive to the exact number of relaxed substrate layers: the difference in energy between keeping the substrate fixed and relaxing three substrate layers was small; around 1 meV or less per surface atom in all of the studied cell dimensions [21].

First, we find that placing an (unstrained) top (1×1) layer in hcp, bridge and atop sites yields energies that are 9.8 and 33.0 and 150.1 meV higher than a (1×1) layer in the fcc sites (roughly consistent with the corresponding numbers from Takeuchi, Chan and Ho cited above).

We then modeled the uniaxially compressed structures, similar to the approach reported in Refs. [22–24]. The range of periodicities, p, was chosen to capture the range of interatomic distances near the threading edge dislocation core. The DFT results are shown in Fig. 5. The surface energies are smaller than that of the unreconstructed (1×1) phase, consistent with the stability of reconstructed phase. The periodicity with minimum surface energy is $17a$, in rough agreement with the experimental value of $\sim 22.5a$ at 300 K [4].

To determine the Morse potential parameters V_0, α, and a_0 we calculated the relaxed energy as a function of p for a discrete set of these parameters. Relaxations were performed with the conjugate gradient method, starting from uniformly compressed configurations. We created an interpolated functional form for the relaxed energy as a function of V_0, α, and a_0 using cubic splines. To determine the optimal values of V_0, α, and a_0, this interpolated functional form was fitted using a least-squares method to the corresponding energies computed with DFT. As shown in Fig. 5, the fit is satisfactory and results in $V_0 = 333.173$ meV, $\alpha = 2.9794$, and $a_0 = 0.9564$. (We find, not unexpectedly, a purely harmonic potential, cannot reproduce this dependence).
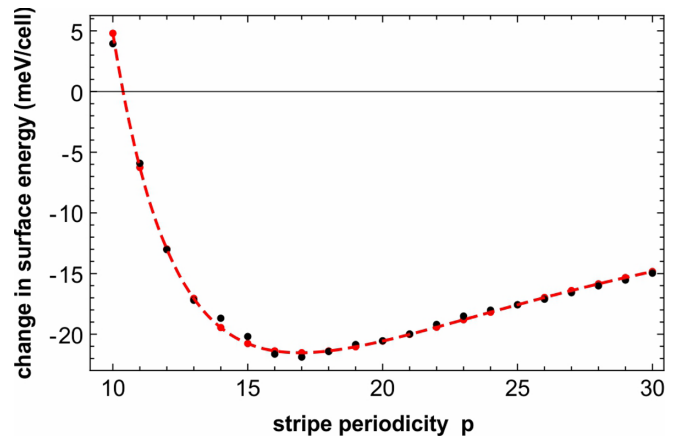

FIG. 5. The surface energy of the uniaxially compressed phase as a function of stripe periodicity p. The black points are results from using density functional theory. The red points are the result of a fit using the Morse potential described in the text. The surface energies are given in units of energy per the (1×1) unit cell of the substrate.

As a further check on the ability of the 2D FK model with the Morse interatomic potential to describe the surface, we compared the structure of the uniaxially compressed phases obtained from DFT to those from the FK model. The plots in Fig. 6 reveal that the atom positions derived with the FK model match those obtained from DFT very well.

Finally, we compare the structure of the elbow computed using our FK model (Fig. 7) with that of the experiment mentioned above and shown in Fig. 3. Our improved FK model now reproduces atomic displacements accurately; the hyperbolic tangent fit gives the elbow width $w = 3.7$, compared to the experimental value of 3.6 ± 0.5. (We note that the FK model does not reproduce well the surface stress. But as previously pointed out in Ref. [11], this is not unexpected because the surface stress necessarily involves processes that distort the substrate, which FK models treat as rigid).

IV. ENERGIES INVOLVED IN THE HERRINGBONE RECONSTRUCTION

After having demonstrated that our FK model can accurately reproduce the DFT values for the atom positions and energy of the stripe phase, as well as the dislocation-core width measured with STM, we will now use this model, with some confidence, to examine the energy of the full herringbone reconstruction, which is currently beyond the reach of DFT due to the large unit cell size. To this aim, we computed the sum of formation energy of the two sorts of threading edge dislocations at the herringbone elbows. This sum is defined as the difference between the energy of the herringbone unit cell and the energy of an equal area of the striped phase. We computed the total formation energy of a pair of the elbow threading edge dislocations, i.e., one "III" type and one "IV" type elbow (see Fig. 1), E_{elbow}, by comparing the energy of our $(14\sqrt{3} \times 102)$ herringbone cell containing 2992 Au atoms with 2992 atoms in a stripe phase of the same density (i.e., one with a $(\sqrt{3} \times 21)$ cell). We find E_{elbow} is still large: 0.77 eV, albeit somewhat less than the value 0.93 eV determined with the harmonic model. Of course the DFT PBE density functional
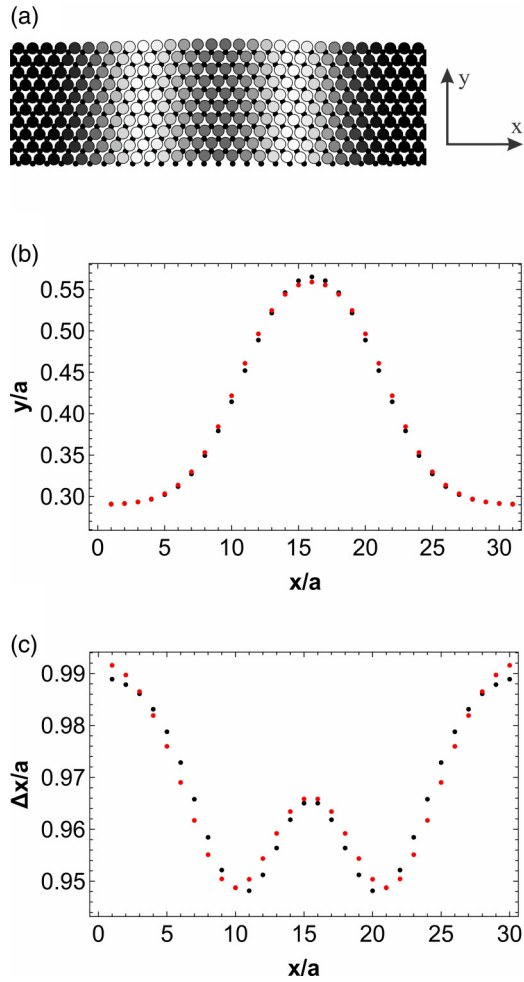
(a)

(b)

(c)

FIG. 6. The displacements of the uniaxially compressed phase computed using density functional theory (black) compared with the predictions of the fitted Morse potential (red). Δx is the x component of the separation between adjacent atoms.

on which our estimate is based has well-known deficiencies (such as underestimating the cohesive energy of Au by 20% [25]). However, our result seems robust: varying V_0, α and $(1-a_0)$ by 10% never decreased the sum of the elbow energies by more than 0.15 meV. Thus, despite the highly inaccurate description of the dislocation core structure of Narasimhan and Vanderbilt, these results support their conclusions that substrate relaxations as described by stress domain theory enable the herringbone reconstruction *if* the 2D FK model is an accurate description of the energetics of the top atomic layer.

Stress domains are expected to form spontaneously when surface relaxations caused by mismatches in surface stress lower the energy by more than the cost of creating boundaries between the stress domains. In this case, the boundaries consist of the lines along the y direction connecting the cores of elbows of the same type, i.e., either those of region III or region IV in Fig. 1. The mismatch in surface stress across the boundaries is proportional to the difference between the components of the surface stress tensor in the direction perpendicular ($\sigma_\perp = \sigma_{yy}$) and parallel ($\sigma_\parallel = \sigma_{xx}$) to
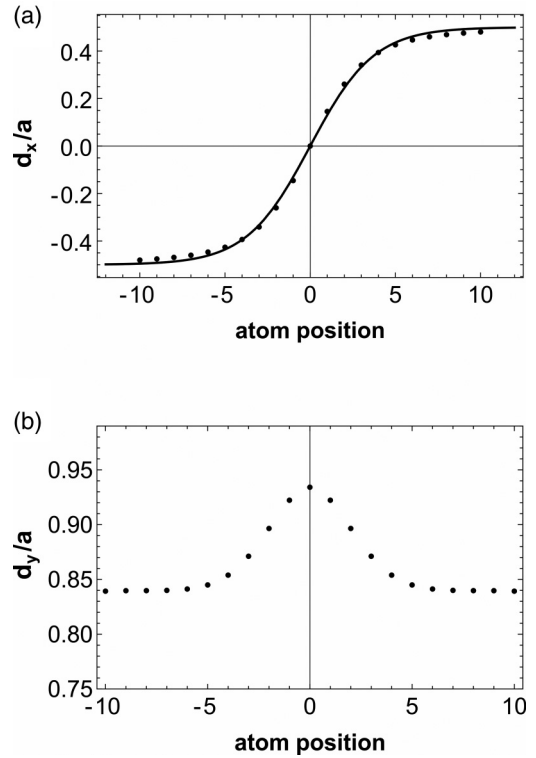

(a)

(b)

FIG. 7. The structure the 2D FK model predicts for the core of the threading edge dislocation. (a) Comparison of the x component of the separation between Au atoms along rows on either side of the dislocation core with experiment. The fit to the hyperbolic tangent gives $w = 3.7$. (b) y component.

the x axis in Fig. 6(a). To estimate the herringbone periodicity, Narasimhan and Vanderbilt used various approximations to estimate $\sigma_\perp - \sigma_\parallel = 105 \pm 20$ meV/Å^2. We have used DFT to compute the surface stress as a function of the periodicity p of the striped phase and plotted the result in Fig. 8. (The surface stresses were determined by comparing the elastic stress tensors of slabs with and without the surface reconstruction). When $p = 17$, the equilibrium value of our DFT calculation, $\sigma_\perp - \sigma_\parallel$ is only 44 meV/Å^2. Such a low value for the stress difference has a significant consequence for the predictions of stress-domain theory [11] for the equilibrium width of the stress domains, i.e., the distance between elbows l_0 along the
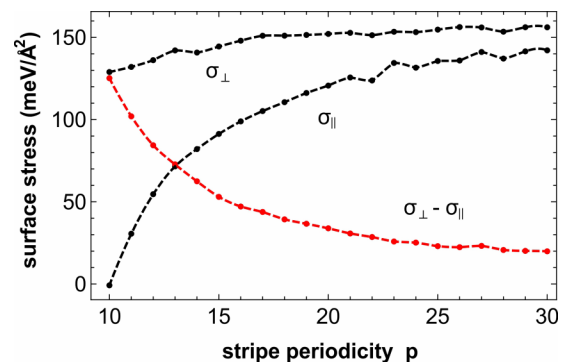

FIG. 8. The variation of the components of the surface stress tensor computed with DFT as a function of stripe periodicity p.
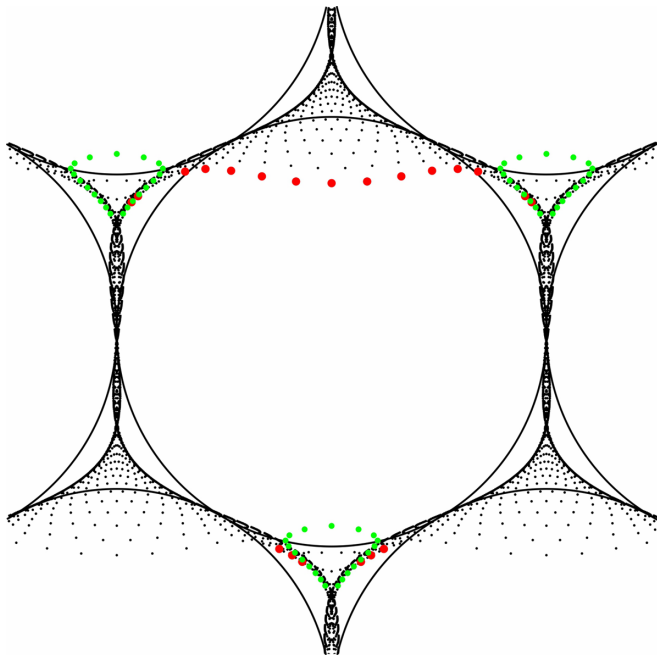
FIG. 9. Each point represents the position, computed with our FK model, of an individual atom in the neighborhood of region IV with respect to the atoms in the unreconstructed second layer (black solid circles). The red and green points mark the positions of the atoms connected by the arrows in Fig. 3(a); the red points represent the lower row of atoms (i.e., those with smaller y), the green points, the upper row.

x direction:

$$l_0 = \pi a_d \exp\left[1 + \frac{E_{\text{elbow}}}{2l_y} \frac{8\pi}{3} \frac{\mu}{(\sigma_\perp - \sigma_\parallel)^2}\right],$$

where l_y is the distance between elbows in the y direction ($14a\sqrt{3}$ in our model), μ (203 meV/Å^3) is given by a combination of elastic constants as specified in Ref. [11] and a_d is the width of the domain walls (estimated by Narasimhan and Vanderbilt to be $3a$ to $8a$, consistent with our value of the elbow width $w = 3.7$). Using the computed values for these parameters, the predicted value of l_0 would be in the range of 7000 to 19000 Å, much greater than the experimental value of $\sim$150 Å. (The model of Narasimhan and Vanderbilt gives a range of 140 to 980 Å). To correct this discrepancy would require E_{elbow} to be 0.11 eV, much smaller than our FK-based estimate of 0.77 eV. We now discuss possible reasons for this discrepancy.

The improved FK model used here still has many unrealistic features. One feature of particular concern is what happens when surface atoms are displaced towards atop sites. In the uniaxially compressed ($\sqrt{3} \times 22$) region, as inspection of Fig. 1 shows, the surface atoms are approximately located on a line connecting the fcc, bridge, and hcp sites, and displacements towards the atop sites are small. This situation is distinctly different for the elbow dislocations. The importance of the atop energy is seen graphically in Fig. 9, where the (FK model-derived) positions of the surface atoms with respect to the substrate atoms are plotted. (Only one elbow type is shown; the other exhibits similar behavior). Clearly,
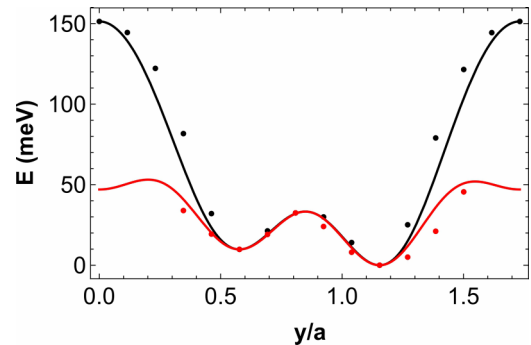

FIG. 10. The black points represent DFT energies of surface atoms displaced along a line in the y direction connecting fcc, hcp, bridge, and atop sites, when the positions of the substrate atoms are fixed. The red points show the corresponding energy values when the atoms beneath the substrate atoms are allowed to relax. The black curve is the fit of Eq. (2) using the calculated values of the fcc, hcp, bridge, and atop site energies. The red curve is the result of Eq. (2) assuming an atop energy of 46 meV.

the atoms near the core are displaced towards the atop site; thus, lowering the atop energy would decrease the dislocation core energy.

Because of their displacements towards the atop sites, the atoms in the elbow dislocation cores create forces in the y direction on the substrate. The long-ranged elastic relaxations of the substrate caused by such forces (as discussed above) can lower the energy sufficiently to stabilize the elbows. However, the existence of these forces also imply that the situation envisioned by the FK model, surface atoms displaced on a rigid substrate, might become unrealistic in the dislocation cores: the forces will necessarily cause the substrate atoms to be displaced vertically as well as laterally as surface atoms are moved towards the atop sites. The parameters for the substrate potential [Eq. (2)], e_t, e_b, and e_h, are DFT energies of highly symmetric configurations which undergo only negligible lateral displacements during relaxation, and might thus not be a proper gauge of the energy cost of lateral displacements away from high-symmetry sites. In fact, the uppermost substrate atoms (directly below the surface atoms) might shift relatively easily from fcc sites towards hcp sites, as they do for the surface relaxations in the stripe phase, thus lowering the energy cost of shifting the atoms directly above them in the same direction (which would be towards on top sites). To estimate the importance of this effect, we recalculated the substrate corrugation of Eq. (2) in DFT by allowing the uppermost substrate atoms to relax. In Fig. 10, the result (red points) is compared with the rigid substrate (black points) along a line in the y direction connecting fcc, hcp, bridge, and atop sites. Clearly the substrate relaxations lower considerably the energy of displacing atoms towards the atop sites.

Given these shortcomings it is clear that our FK model has overestimated E_{elbow}. This prompts us to explore the possibility mentioned in the Introduction, that the elbows could, in principle, have negligible or even negative formation energies within a FK model. To probe how much our model would need to be modified to obtain a small formation energy, we varied the atop site energy in the FK model. For each value of the atop energy we refitted the parameters of the Morse potential
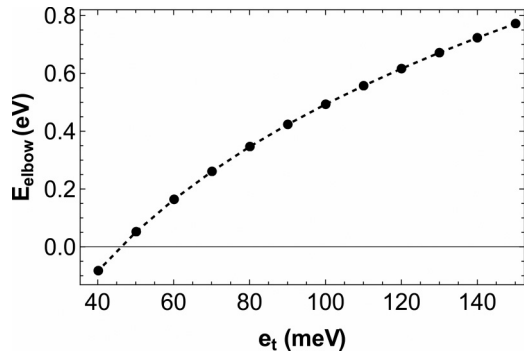
FIG. 11. The formation energies of an elbow pair as a function of the atop energy in the FK model. The dashed line is a guide to the eye.

to the DFT results and recomputed the dislocation core formation energies. The result is shown in Fig. 11. The elbow formation energies become small when the atop energy becomes small. Presumably, a small atop energy (positive) can be overcome by the energy gain (negative) due to biaxial relaxion in the surface layer near the dislocation core, favoring elbowed regions over striped regions, which are only uniaxially relaxed. Figure 11 shows that the dislocation formation energy becomes negative when the atop energy is around 46 meV, considerably smaller than the DFT estimate of 150 meV.

Indeed, as shown by the red curve in Fig. 10, the energy cost of the displacements is reasonably described by Eq. (2) with an energy of $e_t = 46$ meV, the value of the atop energy needed to make the formation energy of the elbow dislocations zero (see Fig. 11). The x and y displacements of the atom positions through the elbow are relatively insensitive to the choice of e_t: the fitted w merely changes from 3.7 to 3.9, still consistent with experiment ($w = 3.6$).

Thus, by adjusting the FK substrate parameters to account for the relaxation of just one atom layer below the surface layer, we arrive at a vanishing formation energy for the herringbone elbows and a structure still consistent with experiment. Because the atoms surrounding the elbow constrain the amount of second-layer relaxation, this procedure overestimates the effect of subsurface relaxation. For example, Fig. 3(a) shows that while the surface atoms in the compressed region of the elbow are displaced (downwards on the page) toward the atop sites of the subsurface atoms (red circles), the less dense regions, on the page above the elbow, are displaced in the opposite direction (albeit by much smaller amounts, as shown in Fig. 9). Thus, a rigid shift of the substrate atoms as envisioned by Fig. 10 would not lower the energy everywhere. Mitigating this effect are relaxations in deeper substrate layers. Evidently, determining the elbow energy precisely would require a three-dimensional model that can accurately reproduce the subsurface structure in a way that goes beyond elasticity theory.

There are still compelling reasons to suspect that stress domain theory is important for understanding the herringbone

reconstruction. The density of elbows is determined by a balance between their formation energy and the strength of the interactions between them. As the formation energy becomes small and the equilibrium distance between elbows becomes large, this balance becomes delicate and requires accurate knowledge of the interaction at long distances. The long-range nature of the interactions in the stress domain theory still provides a compelling source of the interactions. However, interactions caused by the strain fields of near-surface relaxations discussed above and the distortions in the Shockley partial arrangement caused by the elbows would need to be considered as well.

V. CONCLUSION

We have shown that a 2D Frenkel-Kontorova model, appropriately parametrized, can reproduce in detail the experimentally determined atomic structure of a dislocation at an elbow in the herringbone reconstruction. Computing the energy of the elbow dislocations within the 2D model turns out to be quite subtle, because the forces that the surface atoms in the elbow dislocation apply on substrate atoms will necessarily cause significant subsurface displacements. These displacements will clearly depend on atomistic details and thus require more than bulk elasticity theory to be calculated accurately.

This conclusion is reinforced by our DFT calculations of the surface stress tensor of the $\sqrt{3} \times p$ (stripe phase) Au(111) reconstruction. The computed surface stress anisotropy, which according to stress domain theory would lead to the formation of the herringbone reconstruction, is a factor of 2 smaller than previous estimates. As we have shown, to explain the observed herringbone periodicity, this would require an elbow energy roughly a factor of 10 smaller that the simple 2D FK models would predict. Our results indicate that this sort of decrease could be created by relaxations of the second atomic layer.

The possibility of a low formation energy of threading dislocations, such as the one we find for the Au(111) herringbone elbows, can account for their ubiquity in other systems, especially in heteroepitaxy. Our results suggest that caution is warranted in using the 2D FK model to predict the formation of these dislocation: Despite the success of the FK models in reproducing the overall structure and phase diagrams of metal thin film surface structures, their use to quantify subtle energy balances can be problematic.

[1] C. B. Carter and R. Q. Hwang, Dislocations and the reconstruction of (111)fcc metal-surfaces, Phys. Rev. B **51**, 4730 (1995).

[2] K. Thürmer, C. B. Carter, N. C. Bartelt, and R. Q. Hwang, Self-Assembly via Adsorbate-Driven Dislocation Reactions, Phys. Rev. Lett. **92**, 106101 (2004).

[3] W. L. Ling, J. C. Hamilton, K. Thürmer, G. E. Thayer, J. de la Figuera, R. Q. Hwang, C. B. Carter, N. C. Bartelt, and K. F. McCarty, Herringbone and triangular patterns of dislocations in Ag, Au, and AgAu alloy films on Ru(0001), Surf. Sci. **600**, 1735 (2006).

[4] A. R. Sandy, S. G. J. Mochrie, D. M. Zehner, K. G. Huang, and D. Gibbs, Structure and phases of the Au(111) surface - x-ray-scattering measurements, Phys. Rev. B **43**, 4667 (1991).

[5] J. V. Barth, H. Brune, G. Ertl, and R. J. Behm, Scanning tunneling microscopy observations on the reconstructed Au(111) surface - atomic-structure, long-range superstructure, rotational domains, and surface-defects, Phys. Rev. B **42**, 9307 (1990).

[6] D. D. Chambliss, R. J. Wilson, and S. Chiang, Nucleation of Ordered Ni Island Arrays on Au(111) by Surface-Lattice Dislocations, Phys. Rev. Lett. **66**, 1721 (1991).

[7] W. Chen, V. Madhavan, T. Jamneala, and M. F. Crommie, Scanning Tunneling Microscopy Observation of an Electronic Superlattice at the Surface of Clean Gold, Phys. Rev. Lett. **80**, 1469 (1998).

[8] Y. Hasegawa and P. Avouris, Manipulation of the reconstruction of the Au(111) surface with the STM, Science **258**, 1763 (1992).

[9] V. Repain, J. M. Berroir, S. Rousset, and J. Lecoeur, Reconstruction, step edges and self-organization on the Au(111) surface, Appl. Surf. Sci. **30**, 162 (2000).

[10] J. A. Stroscio, D. T. Pierce, R. A. Dragoset, and P. N. First, Microscopic aspects of the initial growth of metastable fcc-iron on Au(111), J. Vac. Sci. Technol. A-Vac. Surf. Films **10**, 1981 (1992).

[11] S. Narasimhan and D. Vanderbilt, Elastic Stress Domains and the Herringbone Reconstruction on Au(111), Phys. Rev. Lett. **69**, 1564 (1992).

[12] J. C. Hamilton and S. M. Foiles, Misfit Dislocation Structure for Close-Packed Metal-Metal Interfaces, Phys. Rev. Lett. **75**, 882 (1995).

[13] C. E. Bach, M. Giesen, H. Ibach, and T. L. Einstein, Stress Relief in Reconstruction, Phys. Rev. Lett. **78**, 4225 (1997).

[14] N. Takeuchi, C. T. Chan, and K. M. Ho, Au(111) - a theoretical-study of the surface reconstruction and the surface electronic-structure, Phys. Rev. B **43**, 13899 (1991).

[15] R. Pushpa and S. Narasimhan, Reconstruction of Pt(111) and domain patterns on close-packed metal surfaces, Phys. Rev. B **67**, 205418 (2003).

[16] S. Mehendale, M. Marathe, Y. Girard, V. Repain, C. Chacon, J. Lagoute, S. Rousset, and S. Narasimhan, Prediction of reconstruction in heteroepitaxial systems using the Frenkel-Kontorova model, Phys. Rev. B **84**, 195458 (2011).

[17] G. Kresse and J. Furthmüller, Efficient iterative schemes for *ab initio* total-energy calculations using a plane-wave basis set, Phys. Rev. B **54**, 11169 (1996).

[18] G. Kresse and J. Furthmüller, Efficiency of *ab in itio* total energy calculations for metals and semiconductors using a plane-wave basis set, Comp. Mat. Sci. **6**, 15 (1996).

[19] G. Kresse and D. Joubert, From ultrasoft pseudopotentials to the projector augmented-wave method, Phys. Rev. B **59**, 1758 (1999).

[20] J. P. Perdew, K. Burke, and M. Ernzerhof, Generalized Gradient Approximation Made Simple, Phys. Rev. Lett. **77**, 3865 (1996).

[21] We find that the periodicity of the striped phase with lowest surface energy does not depend on whether the substrate atoms are relaxed or not. If the surface stress difference between hcp and fcc regions in the stripe phase were large, one might expect significant elastic relaxations in the slab, as observed for example in the case O/Cu(110) in J. Harl and G. Kresse, Density functional theory studies on stress stabilization of the Cu(110) striped phase, Surf. Sci. **600**, 4633 (2006). However the surface stress difference we find between hcp and fcc regions is only 11 meV/Å^2, much smaller than the 81 meV/Å^2 computed for O/Cu(110).

[22] E. Torres and G. A. DiLabio, A density functional theory study of the reconstruction of gold (111) surfaces, J. Phys. Chem. C **118**, 15624 (2014).

[23] Y. Wang, N. S. Hush, and J. R. Reimers, Simulation of the Au(111)-(22 x $\sqrt{3}$) surface reconstruction, Phys. Rev. B **75**, 233416 (2007).

[24] F. Hanke and J. Bjork, Structure and local reactivity of the Au(111) surface reconstruction, Phys. Rev. B **87**, 235422 (2013).

[25] F. Tran, J. Stelzl, and P. Blaha, Rungs 1 to 4 of DFT Jacob's ladder: Extensive test on the lattice constant, bulk modulus, and cohesive energy of solids, J. Chem. Phys. **144**, 204120 (2016).